TITLE

Time evolution of "in vivo" articular cartilage repair induced by bone marrow stimulation and scaffold implantation in rabbits.

AUTHORS

María Sancho-Tello[1,2,3], Francisco Forriol[4], Pablo Gastaldi[4], Amparo Ruiz-Saurí[1,2,3], José J. Martín de Llano[1,2,3], Edurne Novella-Maestre[5], Carmen M. Antolinos-Turpín[6], José A. Gómez-Tejedor[6], José L. Gómez Ribelles[3,6], Carmen Carda[1,2,3]

AFFILIATION

[1] Departamento de Patología, Universitat de València, Spain.

[2] INCLIVA, Valencia, Spain.

[3] CIBER-BBN en Bioingeniería, Biomateriales y Nanomedicina, Valencia, Spain.

[4] Clínica Gastaldi, Hospital Nou d'Octubre, Valencia, Spain.

[5] Hospital Universitari i Politècnic la Fe, Valencia, Spain.

[6] Centro de Biomateriales e Ingeniería Tisular, Universitat Politècnica de València, Valencia, Spain.

PUBLICATION

Int J Artif Organs 2015; 38(4): 210-223

DOI: 10.5301/ijao.5000404

CORRESPONDING AUTHOR

María Sancho-Tello
Facultad de Medicina y Odontología
Departamento de Patología
Universitat de València
Av. Blasco Ibáñez 15
46010 Valencia (Spain)
E-mail: Maria.Sancho-Tello@uv.es
Telephone: (34)963864100
Fax: (34)963983226

The Authors state that this manuscript has not been published previously and is not currently being assessed for publication by any journal other than The International Journal of Artificial Organs.

Each Author has contributed substantially to the research, preparation and production of the paper and approves of its submission to the Journal.

FINANCIAL SUPPORT

This study was supported by the Spanish Ministry of Science and Innovation through MAT2010-21611-C03-00 project (including the FEDER financial support), by Consellería de Educación (Generalitat Valenciana, Spain) PROMETEO/2011/084 grant, and by CIBER-BBN en Bioingeniería, Biomateriales y Nanomedicina. The work of JLGR was partially supported by funds from the Generalitat Valenciana, ACOMP/2012/075 project. CIBER-BBN is an initiative funded by the VI National R&D&i Plan *2008-2011, Iniciativa Ingenio 2010, Consolider Program, CIBER Actions* and financed by the Instituto de Salud Carlos III with assistance from the *European Regional Development Fund*.

CONFLICT OF INTEREST

The authors state they do not have proprietary interest.

MEETING PRESENTATION

This study has been partially presented at the following meeting:
V European Chapter of the Tissue Engineering and Regenerative Medicine International Society (TERMIS) and XVI Meeting of the Spanish Society of Histology and Tissue Engineering (SEHIT). Granada (Spain). June 7-10, 2011. *Histol Histopathol.* 2011; 26(Suppl.1):84-85.

ABSTRACT

Purpose: Tissue engineering techniques were used to study cartilage repair over 12-month period in a rabbit model.

Methods: A full-depth chondral defect along with subchondral bone injury were originated in the knee joint, where a biostable porous scaffold was implanted, synthesized of poly(ethyl acrylate-co-hydroxyethyl acrylate) copolymer. Morphological evolution of cartilage repair was studied 1 and 2 weeks, and 1, 3 and 12 months after implantation by histological techniques. Three-month group was chosen to compare cartilage repair to an additional group where scaffolds were preseeded with allogeneic chondrocytes before implantation, and also to controls, who underwent the same surgery procedure, with no scaffold implantation.

Results: Neotissue growth was first observed in the deepest scaffold pores 1 week after implantation, which spread thereafter; 3 months later scaffold pores were filled mostly with cartilaginous tissue in superficial and middle zones, and with bone tissue adjacent to subchondral bone. Simultaneously, native chondrocytes at the edges of the defect started to proliferate 1 week after implantation; within a month those edges had grown centripetally and seemed to embed the scaffold, and after 3 months, hyaline-like cartilage was observed on the condylar surface. Preseeded scaffolds slightly improved tissue growth, although the quality of repair tissue was similar to non-preseeded scaffolds. Controls showed that fibrous cartilage was mainly filling the repair area 3 months after surgery. In the 12-month group, articular cartilage resembled the untreated surface.

Conclusions: Scaffolds guided cartilaginous tissue growth "in vivo", suggesting their importance in stress transmission to the cells for cartilage repair.

KEY WORDS: Cartilage, Regenerative Medicine, Biocompatible Materials, Tissue Scaffolds, Experimental Animal Models

INTRODUCTION

Articular cartilage is an avascular tissue that has a limited ability to repair in adults (1, 2). It contains an extracellular dense matrix rich in water along with proteoglycan and type II collagen (3), but only about 5% of the tissue volume is occupied by chondrocytes, that are isolated cells embedded in lacunae, responsible for matrix synthesis and turnover, and have no contact with other neighbor cells. Since articular cartilage is free of blood vessels and innervation, nutrients and oxygen supply is constrained to diffusion, which is, however, facilitated by compressive cyclic loading that provides a pumping mechanism during joint movements. When cartilage is injured, cells are unable to leave their territory through the dense matrix, and have little potential to increase their metabolic rate to regenerate neotissue. Thus, the healing response of articular cartilage in adults is very limited in most "in vivo" situations, although cartilage does grow and remodel vigorously during pre- and postnatal development (4, 5).

Orthopedic surgeons have developed several therapeutic strategies in order to resurface the damaged articular cartilage (6), such as tissue response techniques by drilling (7), microfracture (8), osteochondral transplantation (mosaicplasty, 9), and periosteum or perichondrium transplantation (2, 10), which require a reparative or regenerative response by the host site. Clinical results are not always satisfactory, so the results in patients undergoing microfracture are influenced by age, as well as by the type and size of the defect, and thus younger and active patients have the best long-term results (11). On the other hand, mosaicplasty may be limited by the size of the injured area and involves surgical aggression in both the donor and receptor regions of the osteochondral graft.

Cell therapy has also been used for *in situ* cartilage regeneration to promote the formation of articular cartilage, using either autologous chondrocytes or mesenchymal stem cells (2). Cultured chondrocytes demonstrate that "in vitro" conditions may reactivate a significant regenerative potential of chondrocytes. Human autologous chondrocyte transplantation was first proved in 1994 (12), being successfully applied for more than a decade and is considered the gold standard in reparation of osteochondral injuries; however it has major limitations and disadvantages, such as an arthrotomy incision, the need to obtain sufficient cell number to fill large defects, and the fact that patients undergo two surgical operations, among other problems (13). On the other hand, pluripotential mesenchymal stem cells are located in the bone marrow at low concentration, and they can migrate directly to the defect site when bone was injured; the blood clot formed is thought to develop a favorable microenvironment capable of stimulating attraction, proliferation and differentiation towards

various cell types, including chondrocytes and bone cells, making them a potential cell source in osteoarticular repair (11, 13).

In the treatment of cartilage injuries, tissue engineering techniques using scaffolds have led to promising results (6), aiming to regenerate articular defects by using empty scaffolds or scaffolds seeded with autologous chondrocytes (14). Scaffolds rapidly fill cartilage defects and provide a temporary substrate onto which invading cells can adhere. They also play important roles in maintaining mechanical integrity and withstanding mechanical stresses, therefore they should be designed to match mechanical properties with those of native cartilage, as well as appropriate for the loading conditions of the joint (6, 15, 16). Different "in vivo" studies had demonstrated the importance of the stress transmission to the cells in cartilage regeneration. For instance, it was observed that chondrocytes required a minimum amount of stimulation in order to elicit an anabolic response (17). It has also been shown that mechanostimulation of chondrocytes enhanced the growth of a cartilage-like tissue "in vitro" (18) as well as the synthesis of glycosaminoglycan (19) and extracellular matrix (20).

Different studies have tested a range of polyesters to manufacture scaffolds, including polyglycolide, polylactide, poly(*ε*-caprolactone), poly(ethyl acrylate, EA) and their co-polymers, that supported cell attachment, proliferation and matrix production for a variety of cell types, including chondrocytes, osteoblasts and mesenchymal stem cells (21-23). The influence of the hydrophilic/hydrophobic property balance on cell attachment in polymethacrylates has been the subject of several studies. While hydrophilic polymers such as poly(hydroxyethyl methacrylate) and poly(hydroxyethyl acrylate, HEA) are not adhesive for either fibroblasts or other cell lines, hydrophobic polymers of the same series such as poly(methyl methacrylate, PMMA), or poly(ethyl methacrylate), did allow cell anchorage (23-27).

One-step forward in the study of cartilage repair is "in vivo" systems, where the characteristics of the neotissue formed within the engineered constructs can be evaluated. When scaffolds were seeded with rabbit chondrocytes and implanted subcutaneously or within cartilage defects, the differentiation and specific gene expression of chondrocytes was demonstrated (28-32).

Our aim was to study the mechanism of "in vivo" long-term cartilage repair (from 1 week to 12 months), by utilizing tissue engineering techniques when the cell source are mesenchymal stem cells migrating from subchondral bone and invading a synthetic biostable scaffold, implanted without any preseeded cells in the cartilage defect, which maintain mechanical integrity. We used 2-month-old rabbits, which still present cellular

proliferation and reorganization in the articular cartilage (4, 5), and thus neotissue growth was expected at the injury site. Besides, the role of the cell source was studied by comparing the repair process 3 months after implanting scaffolds preseeded with adult chondrocytes. The material employed in this study is a copolymer network made of poly(EA) and HEA, a biocompatible biostable polymer, and thus no interference of degradation material occurred, while mechanical properties throughout the regenerative process were maintained. Our group has previously used these copolymers both "in vitro" an "in vivo" for different applications. For instance, Gómez Ribelles et al. (33) used copolymers based on hydrophobous EA and containing a small fraction of a hydrophylic component for induction joint cartilage regeneration. In addition, poly(EA) copolymers were implanted inside rabbit cornea as a model for a keratoprosthesis (34), whereas scaffolds with aligned channels based on acrylate copolymers were studied as colonizable structures both "in vitro" with neural progenitor cells and "in vivo" (35).

MATERIALS AND METHODS

Polymeric scaffolds

Macroporous scaffolds were copolymer networks made of EA and HEA [P(EA-co-HEA)]. Monomers were EA (Aldrich, 99% pure) and HEA (Aldrich, 96%). Triethyleneglycoldimethacrylate (TEGDMA; Aldrich, 98%) was used as cross-linking agent and benzoine (Scharlau) as ultraviolet (UV) photosensitive initiator.

Scaffolds were prepared using a template made of PMMA microspheres with 90 μm average diameter (Colacryl DP 300, Lucite International) that were sintered under pressure at temperatures above its glass transition temperature, according to the procedure previously described (36). The microspheres were introduced into a mould consisting of two glass plates separated by a rubber ring. The mould was placed into a hot press at 170 ºC to allow PMMA microspheres to soften, and then compressed to form a template of approximately 2 mm thickness. The interconnection points between porogen microspheres create the pore throats in the scaffold (pores of 90 μm diameter, as the template used); thus, pore interconnectivity is controlled by the pressure applied when producing the template.

Templates were immersed in the monomeric solutions including a 5% weight TEGDMA as cross-linker and 1% weight of benzoine as photoinitiator and polymerized under UV light at

room temperature. After polymerization, the template was dissolved with acetone for approximately 48 h in a Soxhlet extractor. Then, scaffolds were immersed in a large excess of acetone and the solvent was slowly changed to water in order to avoid the collapse of the scaffolds. Replicas of the scaffolds were cut in slices of approximately 3 mm diameter and 1 mm thickness. Then, scaffolds were dried in vacuo for 24 h at room temperature following by 24 h at 50 ºC, and they were finally sterilized with gamma radiation (25 kGy) before used.

Copolymers were prepared to contain 90% EA and 10% HEA by weight. These scaffolds are slightly hydrophilic and thus bulk polymers are able to absorb 2.3 and 3.3% of water measured on dry basis when immersed in liquid water until equilibrium (27).

Scaffold porosity was determined from the differences between the weights of dry samples and samples whose pores were filled with water. In order to assure that water penetrated in all the interconnected pores, dry samples were introduced in a glass vessel at a high vacuum, and water was injected into it (37). Volume fraction of pores in the scaffolds was 0.75 ± 0.03 in all samples.

Scaffold morphology was examined by scanning electron microscopy (Fig. 1). Dry scaffold samples were fractured in liquid nitrogen, mounted on copper stubs, and gold sputtered. The samples were observed with a JEOL JSM5410 scanning microscope under an acceleration tension of 15 kV.

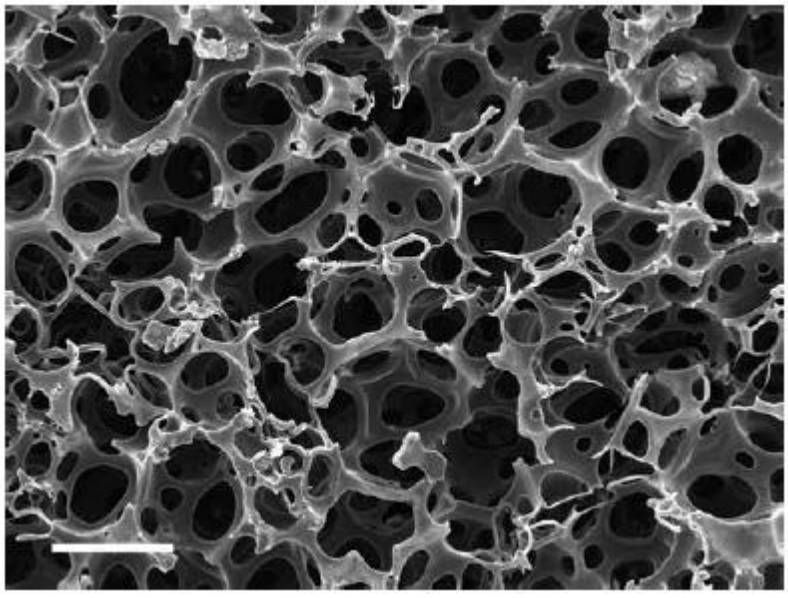

Fig. 1 - Scanning electron microscope picture of a scaffold before implantation. Scale bar represents 100 μm.

Mechanical properties of the biostable porous scaffolds

Compressive strength measurement was carry out in a Termo-Mechanical Assay machine (TMA) Seiko TMA/SS6000 EXSTAR (Japan) in control position mode. Initially, a strain of 2% was applied for 15 min in order to adapt the sample surfaces to the probe. Afterwards, four successive programs of compression to 15% strain and uncompression to initial 2% strain with a rate of 20 µm/min were performed at room temperature. The samples were tested in both dry conditions and immersed in water. The apparent Young modulus was calculated from the slope of the stress-strain curves in the linear region. The results are expressed as the average value of 5 measurements with its corresponding standard deviation (mean±SD).

Animals

Two-month-old male New Zealand rabbits, weighing 1.5-2.0 kg were obtained from Granjas San Bernardo S.L. (Tulebra, Spain) and kept under conventional housing conditions. Quarantine lasted 7 days. Animals were housed with appropriate bedding and provided free access to drinking water and food. Rabbits were kept in standard single cages under controlled temperature and light conditions.
Spanish guidelines for the care and use of laboratory animals have been observed. The study protocol was approved by the Ethics Committee of the Universitat de València according to 86/609/EEC law and 214/1997 and decree 164/1998 of Generalitat Valenciana Government.

Scaffold implant

Rabbits were preanesthetized by subcutaneous injection of 15 mg/kg Ketamine (Ketolar®, Pfizer laboratories) and intramuscular injection of 0.1 mg/kg Medetomidine (Domtor®, Pfizer laboratories), and prepared before surgery (washed, shaved, etc.). Then, general anesthesia was induced by 4% isofluorane using a specially designed mask and maintained by administration of 1.5% isofluorane with O_2 (2 l/min). The surgical site was sterilized using iodine solution and rabbit non-sterile parts were covered with sterile drapes. Surgeons wore sterile coats and gloves, and all instruments were sterilized and kept sterile during surgery. Non-preseeded scaffolds were moistened with phosphate buffered saline (PBS), and vacuum was applied to assure liquid penetration into the pores before implanting.

An arthrotomy at the knee joint was performed through a medial longitudinal parapatellar incision. The medial capsule was incised and the patella laterally dislocated. A 3-mm steel trephine was used to create a 3-mm diameter and about 1-mm depth defect in the central articular surface of the femoral trochlear groove, which resulted in the removal of articular cartilage along with subchondral bone injury. The defect was cleaned and rinsed with sterile saline, and scaffolds were laid into the defect, aligned to surrounding articular surface. Blood was allowed to flow inside scaffolds, which were held in place by repositioning the patella within the femoral trochlear groove. Control animals were subjected to the same operation but no scaffold was implanted in the cartilage defect. Arthrotomy and skin were sutured with continuous stitches of 4/0 Coated Vicryl® (Johnson-Johnson Intl). Macroscopic pictures were taken throughout the surgical procedure to all animals, using a Leica DC150 camera. After removal of the conformed anesthesia mask, rabbits were returned to their cages and allowed free activity in the cage. Postoperative analgesia consisted of intramuscular injection of 3 mg/kg Dexketoprofen (Enantyum®, Menarini laboratories) on the surgery day and the same dose every 24 h for 3 days. At the end of surgery, 3 mg/kg intramuscular injection of Gentamicine (Genta-Gobens®, Normon laboratories) was administered as antibiotic prophylaxis.

Rabbit chondrocyte harvesting and culture

Articular cartilage was obtained from knee joints of donor rabbits after their sacrifice with a lethal intravenous injection of anesthetic overdose in the auricular vein (500 mg/iv Tiopental; Tiobarbital®, Braun laboratories). Chondrocyte isolation and culture was carried out as previously published (23).

Briefly, cartilage was dissected from subchondral bone, finely diced and washed with Dulbecco's modified Eagle's medium (DMEM; Life Technologies) supplemented with 100 U penicillin, 100 µg streptomycin (Biological Industries) and 0.4% fungizone (Gibco). In order to isolate chondrocyte, diced cartilage was successively digested using supplemented DMEM and different enzymes. First, cartilage was incubated for 30 min with 0.5 mg/ml hyaluronidase (Sigma-Aldrich) in a shaking water bath at 37 ºC. Then, hyaluronidase was removed and 1 mg/ml pronase (Merck, VWR International SL) was added. After 60 min incubation in a shaking water bath at 37 ºC, cartilage pieces were washed with supplemented DMEM. Medium was removed and digestion continued by the addition of 0.5 mg/ml of collagenase-IA (Sigma-Aldrich), incubated overnight in a shaking

water bath at 37 ºC. The resulting cell suspension was filtered through a 70 µm pore nylon filter (BD Biosciences) to remove tissue debris. Cells were centrifuged and washed with DMEM supplemented with 10% fetal bovine serum (FBS; Invitrogen). Finally, isolated cells were immediately used for chondrocyte culture.

Isolated cells were plated in culture flasks (T75; Becton-Dickinson) at high density in culture medium (DMEM supplemented with 10% FBS and 50 µg/ml ascorbic acid; Sigma-Aldrich) at 37 ºC in a 5% CO_2 humidified atmosphere, as previously published (23). Medium was changed every 2-3 days. After 7-14 days, adherent cells were harvested by incubation with trypsin-EDTA (Biological Industries), resuspended with a minimum volume of culture medium and counted. Synthetic scaffolds were placed on a 24-well polystyrene culture plate (Nunc A/S) and moistened with Hanks' Balanced Salt Solution (Sigma-Aldrich). After removing excess of Hanks' solution, cell suspension (10^6 viable cells in 20 µl medium) was injected in the center of some of the scaffolds to allow cell infiltration into the porous structure. After 1 h incubation, scaffolds were changed to a new well and culture medium was gently added to ensure that the material was covered. After 3 days in culture, medium was replace by DMEM containing 1% Insulin-transferrin-sodium selenite media supplement (BD Biosciences) and 50 µg/ml ascorbic acid, and preseeded scaffolds were cultured during 3 more days before implanting to animals (3-month preseeded group).

Animal sacrifice and tissue retrieval

Animals with non-preseeded scaffolds were randomly distributed into 5 groups, and were sacrificed at 1 and 2 weeks, and 1, 3 and 12 months after implantation. Since superficial cartilage was repaired 3 months after implantation in most animals, this time point was chosen to compare with an extra group consisted of animals in which preseeded scaffolds were implanted, as well as to control animals, being both groups also sacrificed 3 months after surgery. The number of animals per group is detailed in Table 1.

At the corresponding time after implantation, rabbits were sacrificed as described above. Knee articular cartilage was observed and macroscopic pictures were taken, as mentioned above. Special care was taken in order to keep the repaired defect at the center of the sample in order to asses cartilage repair by histological techniques.

Histological studies

Morphology was studied following standard histological procedures. Briefly, rabbit articulation specimens were rinsed with PBS and fixed with 4% formaldehyde at room temperature for 5 days. Then, samples were rinsed with PBS and immersed in Osteosoft decalcifier solution (Merck) during 5 weeks at room temperature. Specimens were cut through the middle of the scaffold (where the scaffold diameter measured approximately 3 mm), and each half was separately embedded in paraffin. Five-µm thick sections were obtained and stained with hematoxylin-eosin and Masson's trichrome. The ability of chondrocytes to synthesize glycosaminoglycan within the porous scaffold was monitored by alcian blue staining (pH 2.5), counterstained using Harris hematoxylin. Stained sections were analyzed under Leica optical microscope (Leica DM 4000B), and pictures were taken using a camera (Leica DFC 420).

Immunohistochemistry

Standard immunohistochemistry techniques were performed to detect collagen type II, osteocalcin and Ki-67 expression. Monoclonal mouse anti-collagen II antibody (Calbiochem) at 1:200 dilution, incubated at 4 ºC overnight, was used to study the synthesis of collagen type II. Rabbit cartilage areas surrounding the scaffold were used as positive control. Osteocalcin detection was performed using a monoclonal mouse anti-osteocalcin antibody (R&D Systems) at 1:100 dilution, incubated at 4 ºC overnight. Rabbit subchondral bone was used as positive control. Monoclonal mouse anti Ki-67 antibody (MIB-1, DakoCytomation) at 1:50 dilution, incubated at room temperature during 60 min, was employed to detect proliferating cells. Section of human neuroblastoma was used as a positive control. As a negative control for each specific staining, the preimmune serum was substituted for the primary antibody.

Sections were deparaffined and rehydrated through graded ethanol, rinsed in distilled water and treated with 0.3% H_2O_2 and 10% normal horse serum to block endogenous peroxidase and nonspecific binding, respectively. Antigen retrieval for collagen type II and Ki-67 was performed by pressure cooker boiling for 3 min in 10 mmol/L of citrate buffer (pH 6.0). For osteocalcin detection, the slides were permeabilized using 0.1% Triton X-100 for 5 min and antigen retrieval was performed using 0.5% trypsin for 30 min at 37 °C in a humidified chamber. Envision amplification system Dako (CytomationEnvision+System labeled polymer-HRP anti-mouse) was used, followed by revelation with 3,3'-diaminobenzidine (Dako) as chromogen according to the manufacturer's instructions,

which originated a brown staining in immunoreactive structures. Sections were finally counterstained with Mayer's haematoxylin (Sigma).

RESULTS

Mechanical properties of the biostable porous scaffolds

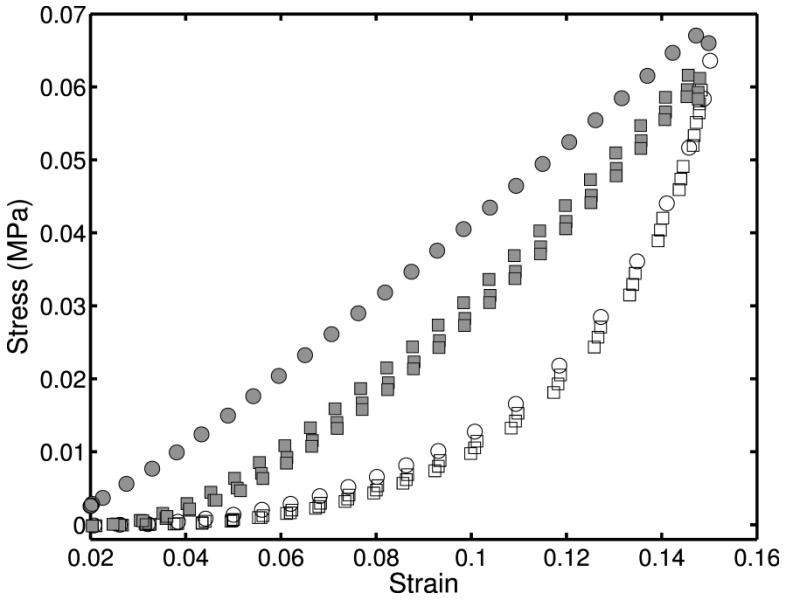

Fig. 2 - Stress-strain curves of the first **(circles)** and following **(squares)** compression and decompression curves in dry conditions. The **gray-filled symbols** represent the compression curves and the **open symbols** the decompression curves.

An example of the stress-strain curve for the porous scaffolds is shown in Figure 2. The first stress-strain curve is different to the other curves that can be attributed to the Mullins effect, also called softening by deformation (38, 39). After the first cycle, the stress-strain curves are practically identical, and a small permanent deformation can be observed in the curves, which could be attributed to plastic deformation of the trabeculae and microfractures of the material with the collapse of some pores.

The apparent Young's modulus was obtained from the slope of the stress-strain curve in the linear region of the compression curve, and it was 0.57±0.10 MPa for the dry samples and 0.34±0.07 MPa for the immersed samples. This result is very similar to the reported values of 0.41±0.12 MPa for the Young's modulus in rabbits (30) and 0.58±0.17 MPa in humans (40).

When a macroporous scaffold is implanted in a tissue, its porous structure is first filled with physiological fluid and then gradually with newly formed tissue. The role of water filling the pores can be an important factor in the mechanical behavior in compression. In this case,

due to the high porosity, the water can flow outwards the samples, and then, the main contribution of the water is a decrease in the compression modulus due to the plasticization effect of the water absorbed in the polymer.

Morphological study

The evolution of the implanted scaffolds was studied by histological techniques throughout a 12-month period, and they were examined at 1 and 2 weeks, and 1, 3 and 12 months after implantation. In general, scaffolds were progressively shifted from the articular surface towards subchondral bone (Fig. 3, macroscopic view) while they were invaded by cells that formed neotissue, which filled a large fraction of the pore volume; in parallel to this process, native articular cartilage proliferated from the edge of the excavated area and formed a neocartilage that regenerated the condylar surface defect (Fig. 4, microscopic view).

Macroscopic analysis

Macroscopic observation of the samples showed that at early stages after implantation (1 week), scaffolds remained aligned to native articular cartilage, contacting with subchondral bone, and no signs of integration with surrounding tissue were observed; on the contrary, scaffolds were delimited by a sharp bloody line (Fig. 3a), which gradually disappeared thereafter. By 1 month after implantation, native articular cartilage seemed to have proliferated surrounding the perforated cavity, causing the scaffold to sink slightly. Three months after implantation scaffolds were easily observed; they showed continuity with the surrounding tissues and were no longer aligned to native articular surface, since they were covered by a layer of cartilage on the surface and also by bone tissue between cartilage and the scaffold in 6 of 8 of the samples (Fig. 3b); when subchondral bone covered scaffolds, a cartilage-like band seemed to link scaffolds with superficial articular cartilage in 3 of 8 of the samples. Twelve months after implantation scaffolds were more difficult to observe since they were mimicking their surrounding and thus a good integration with subchondral bone tissue was observed (Fig. 3c). Figure 3d shows the articular surface 3 months after scaffold implantation; the appearance of the implant site (which can be detected by a slightly lighter color than the surroundings) is very good with a smooth surface, since the scaffold is covered by a regenerated tissue layer, as described above.

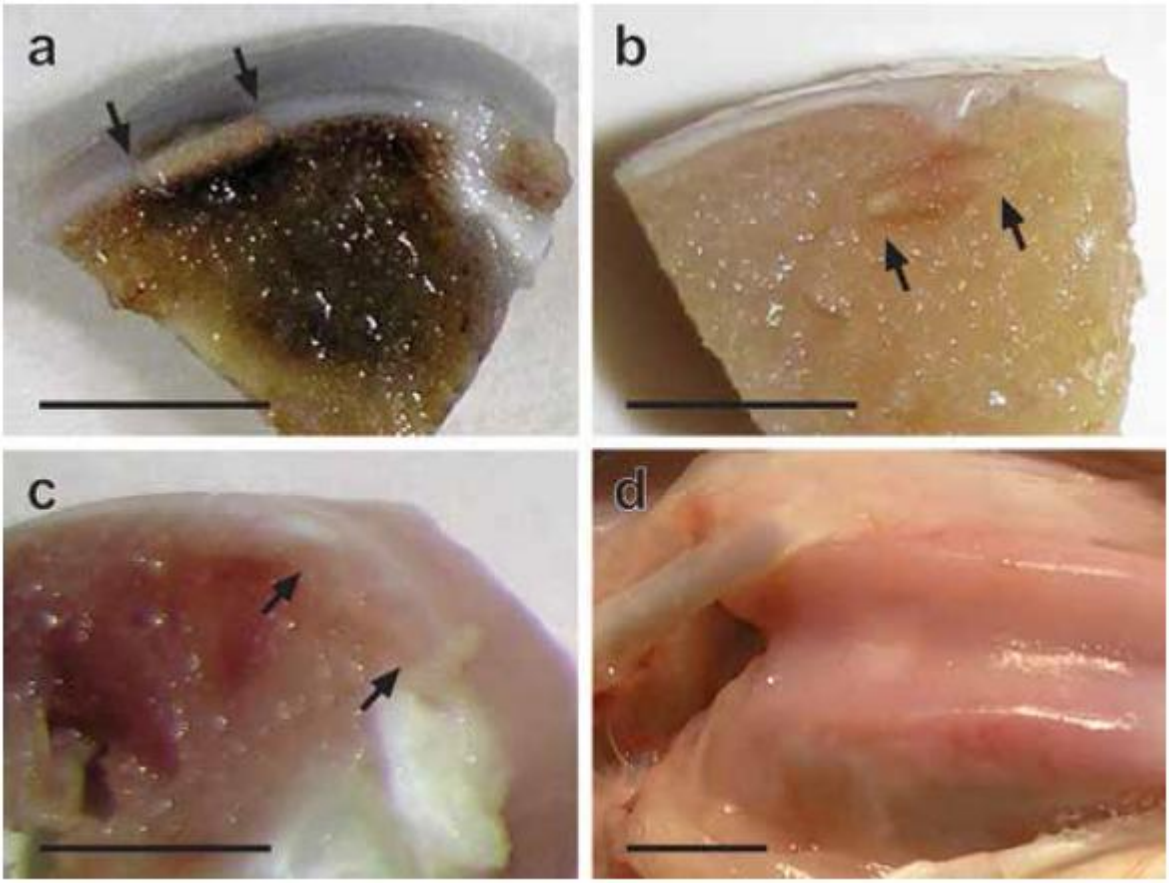

Fig. 3 - Macroscopic view of scaffolds at 1 week **(a)**, 3 months **(b),** and 12 months **(c)** after implantation. Arrows indicate scaffold edges. Articular surface 3 months after scaffold implantation **(d)**. Scale bars represent 5 mm.

Microscopic analysis

Microscopic study revealed that scaffolds showed a progressive shift from articular surface at the earliest stages (Fig. 4a), towards subchondral bone at 3-12 months after implantation (Fig. 4b, c), as macroscopically observed.

The polymeric material did not stain in these samples included in paraffin, and therefore it was observed as white spaces. It remained unaltered throughout the first 3 months after implantation without any sign of degradation, although a slight thinning and deformation of the scaffolds was observed 12 months after implantation (Fig. 4c).

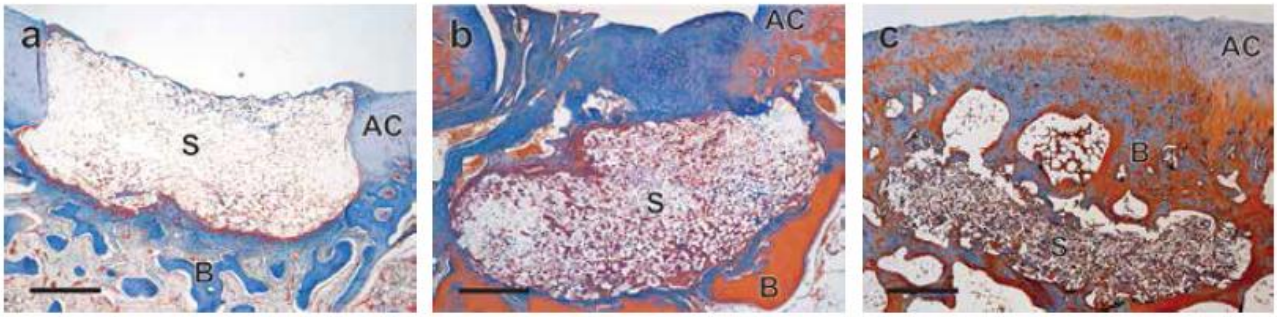

Fig. 4 - Microscopic view of scaffolds 2 weeks **(a)**, 3 months **(b),** and 12 months **(c)** after implantation. 5-micron sections were stained with Masson's trichrome. AC = articular cartilage; B = subchondral bone; S = scaffold. Scale bars represent 500 μm.

1. Articular surface

At the earliest stages after implantation (1-4 weeks), scaffolds appeared at the surface of the defect. By the second week after implantation, a thin layer of amorphous tissue was already observed in most samples covering their surface (Fig. 4a, 5a), that probably arrived from synovial cells. One month after implantation, a well delineated layer of cell-enriched tissue was observed covering all scaffolds (Fig. 5b), that remained aligned with condylar surface.

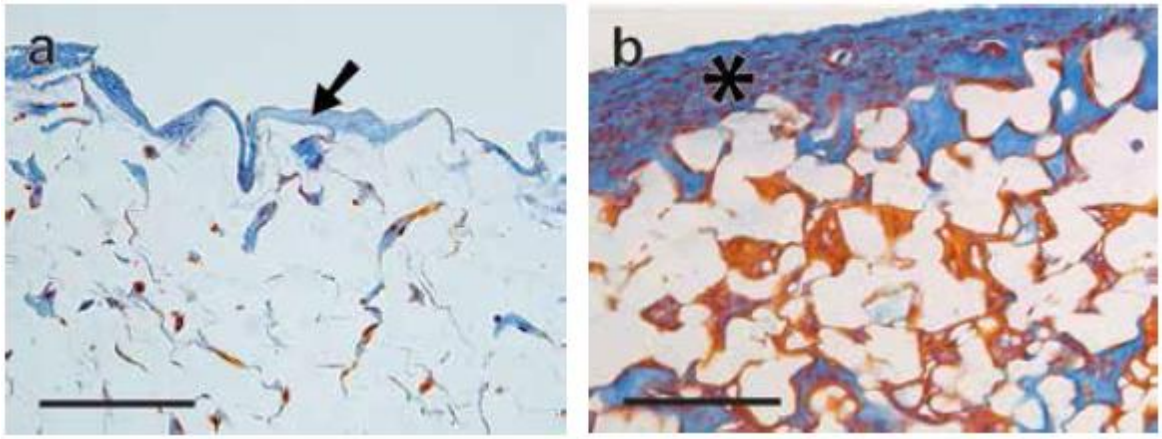

Fig. 5 - Scaffold surface. A thin layer of amorphous **(a, arrow)** or a well delineated cell-enriched layer **(b, asterisk)** tissues were observed covering scaffold surface, 2 weeks or 1 month after implantation, respectively. 5-micron sections were stained with Masson's trichrome. Scale bars represent 100 μm.

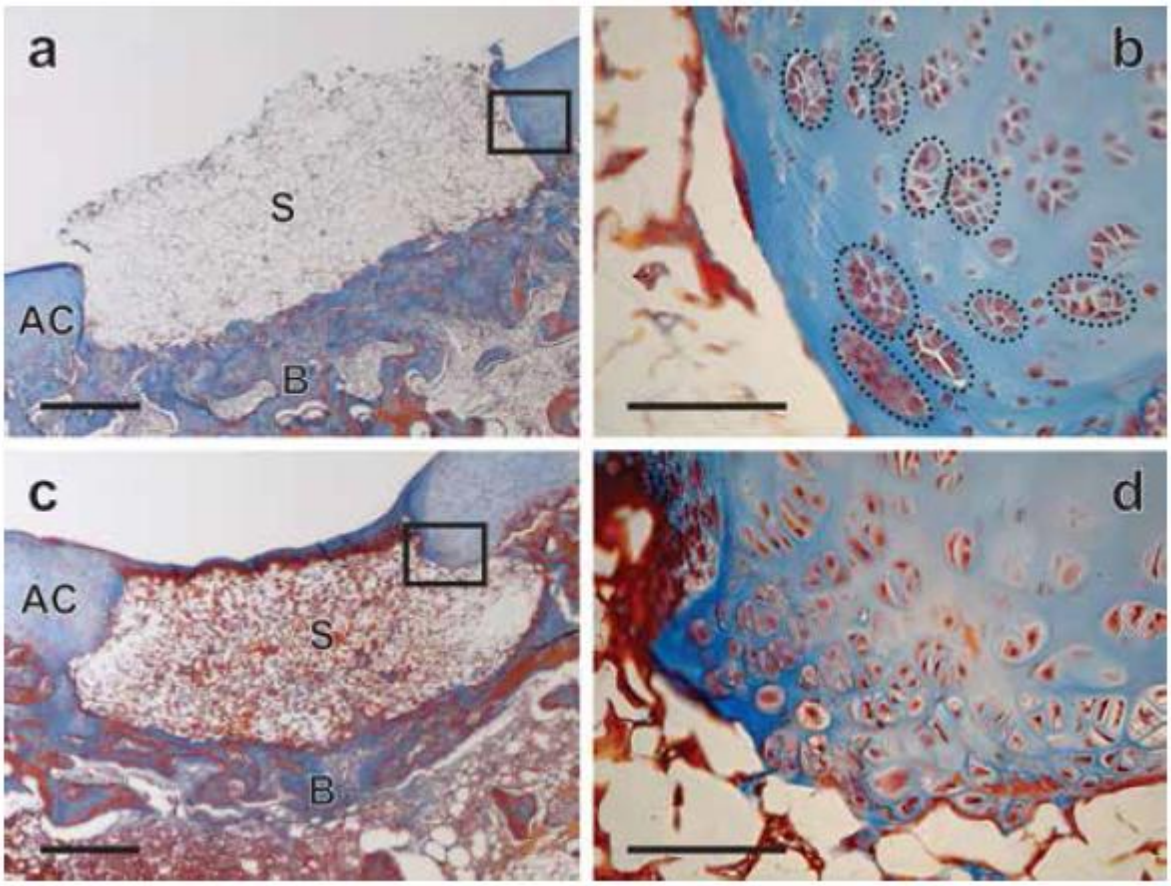

Fig. 6 - Host cartilage edges after scaffold implantation. 1 week after implantation **(a, b)** chondrocyte proliferation was observed in lacunae **(b, dashed circles)** at the edge of the native cartilage, which had grown towards the center of the excavation at 1 month **(c, d)**; b and d are insets of a and c, respectively. 5-micron sections were stained with Masson's trichrome. AC = articular cartilage; B = subchondral bone; S = scaffold. Scale bars represent 500 μm **(a, c)** or 100 μm **(b, d)**.

Meanwhile, the superficial host cartilage began a repair process by activating the chondrocytes located near the edge of the excavated tissue. As soon as 1 week after implantation, lacunae in the native cartilage showed an increased size and proliferation of chondrocytes, with the appearance of more than ten cells inside some lacunae (Fig. 6a, b). Along the time studied, the neocartilage matrix formed was growing centripetally from the edge of the excavated native cartilage towards the center, so that it seemed to be pushing the scaffold towards subchondral bone (Fig. 6c, d). Therefore, 3 months after implantation 6 of 8 samples showed that the growing neocartilage had arrived to the center of the excavated area, contacting and merging with the opposite edge, thus covering the whole scaffold surface at this time (Fig. 7a-c) and partially in the other 2 of 8 samples. Small areas of fibrous cartilage (Fig. 7b) were observed in 2 of 8 samples at this time point. Twelve months after implantation, all samples studied showed an excellent cartilage

repair, with a well-organized layer of hyaline-like cartilage on the top of scaffolds (Fig. 7d), similar to non-treated cartilage.

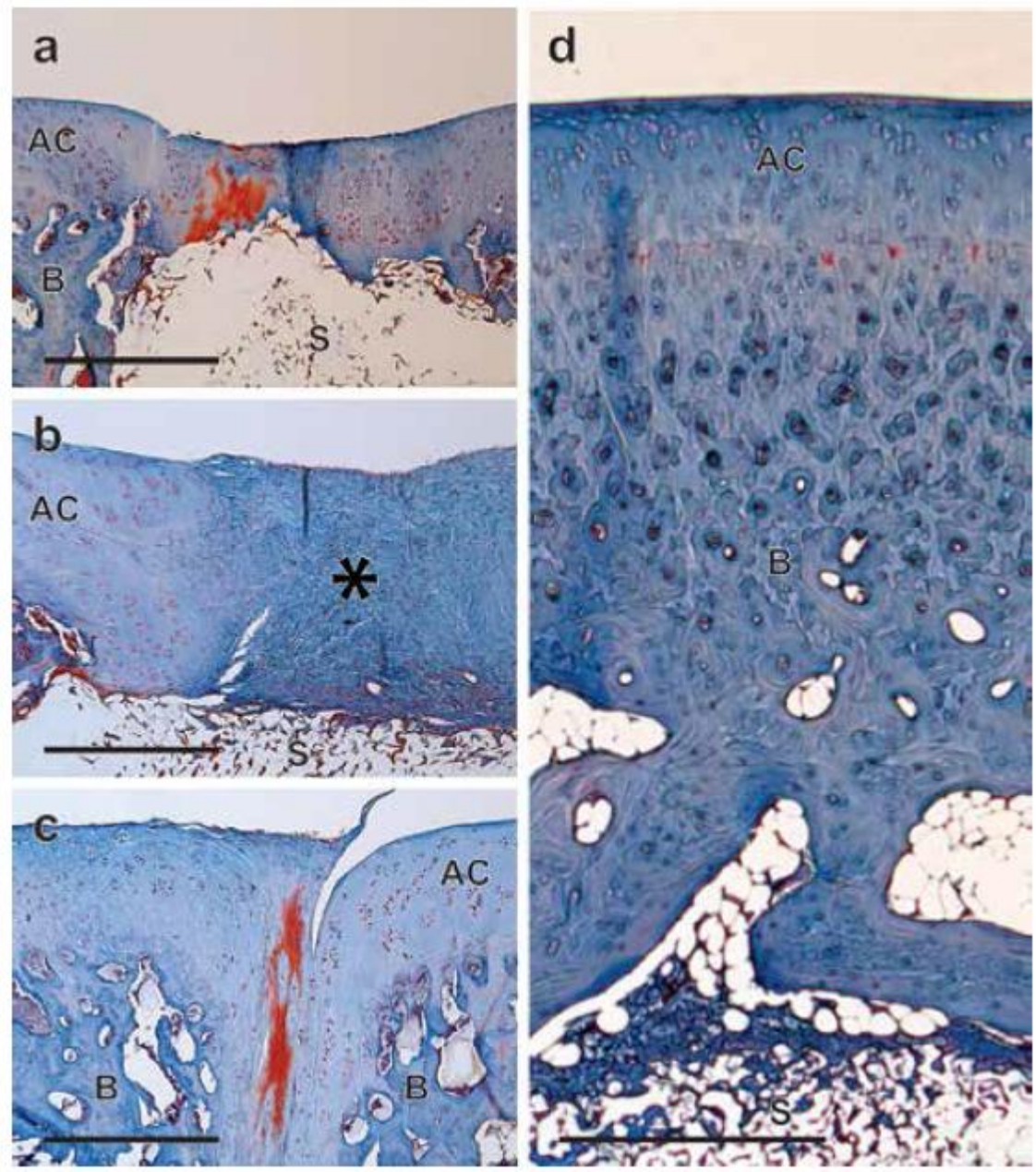

Fig. 7 - Different samples showing superficial neocartilage growth 3 months after implantation, with growing cartilaginous edge **(a, b)** or merging at the center **(c)**, that occasionally was fibrous cartilage **(b, asterisk)**. 12 months after implantation, articular cartilage showed normal architecture and scaffold was covered by subchondral lamellar bone **(d)**. 5-micron sections were stained with Masson's trichrome. AC = articular cartilage; B = subchondral bone; S = scaffold. Scale bars represent 500 μm.

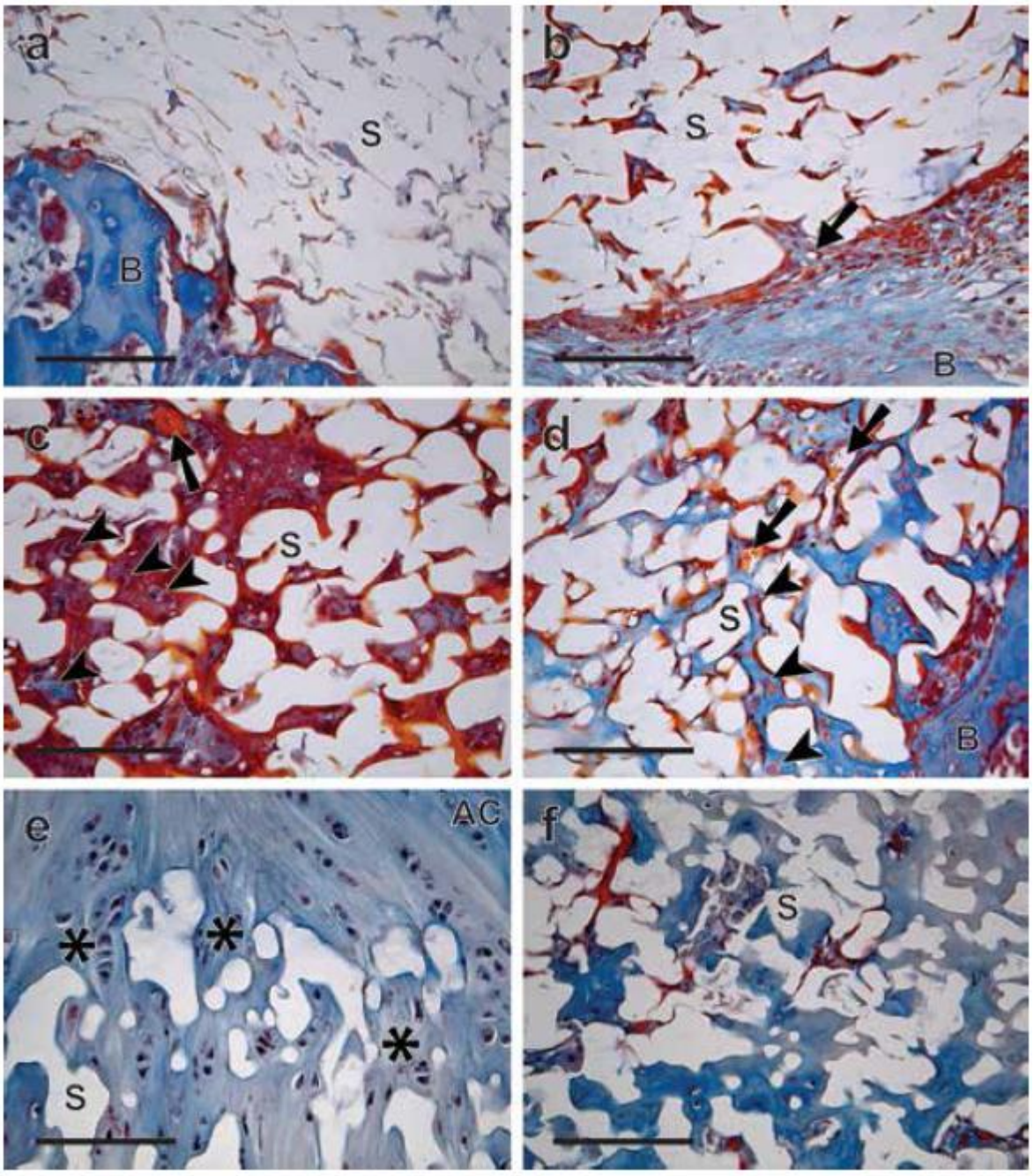

Fig. 8 - Neotissue formation within scaffold pores. Neotissue was scarce 1 week after implantation **(a)**, increased at 2 weeks **(b)**, and was more abundant 1 month after implantation **(c, d)**. 3 months after implantation, cartilaginous **(e)** and bone **(f)** tissues were identified mainly near the superficial and deeper zones of the scaffold, respectively. **Arrows** show capillaries, and **arrowheads** show morphologically differentiated round cells. **Asterisks** show the continuity between neotissue grown inside scaffold pores and native tissue. 5-micron sections were stained with Masson's trichrome. AC = articular cartilage; B = subchondral bone; S = scaffold. Scale bars represent 100 μm.

2. Nesting cells

At the same time that neocartilage was growing on the surface, incipient tissue formation could be observed within scaffold pores from the earliest stages after implantation, which was likely the result of differentiation of mesenchymal cells arriving from subchondral bone marrow. Neotissue formation started 1 week after implantation in the pores located in the deepest zone of the scaffold (Fig. 8a), and spread out throughout the scaffold, arriving to the superficial zone by 1 month after surgery. The amount and type of neotissue formed varied over time and with the location within the scaffolds. At the beginning, few fibroblast-like, morphologically undifferentiated cells were observed within pores, surrounded by scarce amount of homogeneous non-fibrous extracellular matrix (Fig. 8a). By 2 weeks after implantation, increasing number of undifferentiated cells was observed within the pores along with small capillaries, which were occasionally observed emerging from subchondral bone (Fig. 8b). One month after implantation, the newly formed tissue showed signs of morphological differentiation, with a round-cell shape, and a more abundant extracellular matrix that occupied more extensive pore areas than that previously observed (Fig. 8c, d). By the third month after implantation, scaffold pores were apparently filled mostly with cartilaginous tissue in the superficial and middle zones of the scaffold (Fig. 8e), as revealed by alcian blue staining (not shown) and type II collagen immunostaining (Fig. 9a), whereas bone tissue seemed to be the predominant in the deeper zone, adjacent to the subchondral bone (Fig. 8f and 9b). Abundant proliferating cells were observed at this time, as could be checked by Ki-67 immunostaining (Fig. 9c). Twelve months after implantation, when scaffolds were located at great distance from the articular surface (Fig. 4c and 7d), bone was the predominant tissue observed infiltrating scaffolds.

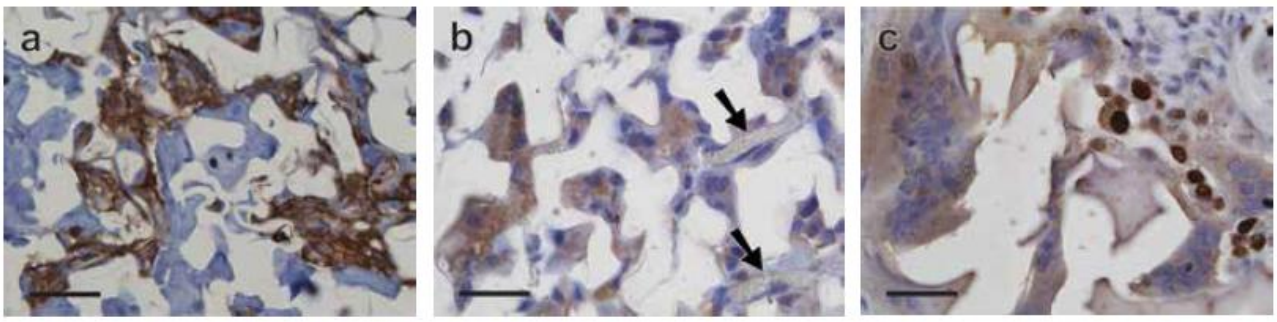

Fig. 9 - Immunohistochemical characterization of neotissue grown inside scaffold pores 3 months after implantation. Hyaline cartilage matrix was characterized by type II collagen immunostaining **(a)**, and bone tissue by osteocalcin immunostaining **(b)**. Proliferative cells observed within

scaffolds were revealed by Ki-67 immunostaining **(c)**. All immunoreactive structures are observed as brown staining. Arrows shows capillaries. Scale bars represent 100 μm.

3. Surroundings

Scaffold integration in the surrounding tissue started as soon as mesenchymal cells invaded scaffold pores (Fig. 8a, b). Three months after implantation, when scaffolds were fully included in the joint tissue and the articular surface was repaired, scaffolds were partly integrated into the surrounding tissue, with continuity between the neotissue grown inside the scaffold pores and the surrounding native tissue, in about 50% of their outlines (Fig. 8e). No necrosis was found, but occasionally, areas of fibrous, inflammatory or reactive tissues, containing leucocytes or phagocytic cells, were also observed surrounding smaller areas (about 20% of their outlines) in 5 of 8 scaffolds (data not shown). Twelve months after implantation, scaffolds were surrounded by spongy bone with microscopic characteristics of lamellar bone tissue (Fig. 7d).

4. Preseeded scaffolds

The repair tissue obtained 3 months after implantation was compared with that obtained when scaffolds were preseeded with allogenic chondrocytes. In this case, scaffolds behavior resembled non-preseeded ones, since they were also located at certain distance from the articular surface, the superficial cartilage was similarly regenerated, and the integration with its surroundings looked like the non-preseeded samples. Subchondral bone covered the entire scaffold upper surface in 1 of 5 samples, and only 25-50% of that surface in the other 4 samples (Fig. 10). Moreover, the quality of the tissue grown inside scaffold pores was similar, although preseeded scaffolds seemed to have a higher proportion of neotissue filling their pores (Fig. 10).

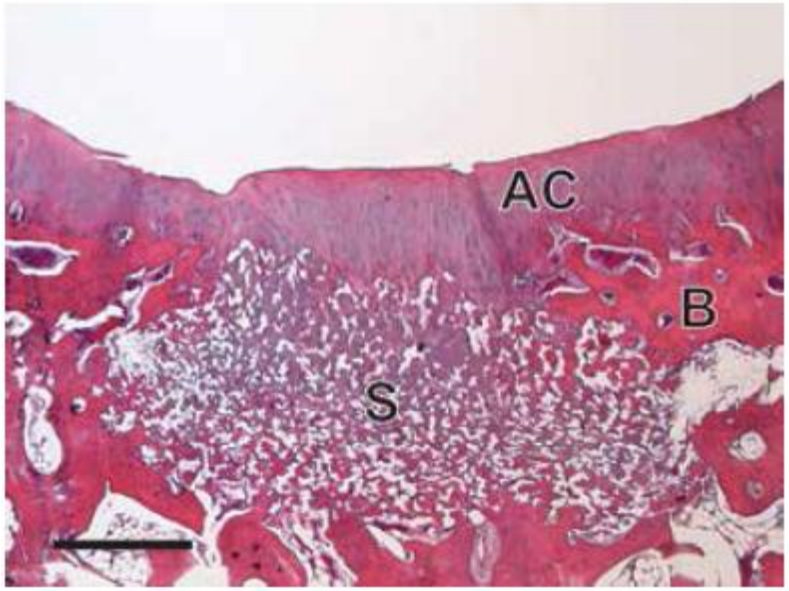

Fig. 10 - Preseeded scaffold 3 months after implantation, in which an abundant neotissue filled scaffold pores while good integration with surrounding tissue was observed. 5-micron sections were stained with hematoxylin-eosin. AC = articular cartilage; B = subchondral bone; S = scaffold. Scale bar represents 500 μm.

5. Control group

Three-month group was chosen to compare cartilage repair to controls, which underwent the same surgery procedure, but without scaffold implantation in the chondral defect. Histological study of the tissue formed in the control animals showed the typical aspect of the regenerated cartilage after microfracture or analogous procedures to injure subchondral bone and allow bleeding into the cartilage defect (41). Articular surface looked rough and irregular macroscopically, whereas disorganized cells were observed under microscope filling the excavated cavity, distributed in an extracellular matrix with a fibrous cartilage aspect (Fig. 11); however, no appearance of growing edges was observed at the host cartilage, as it was observed in the scaffold-implanted samples.

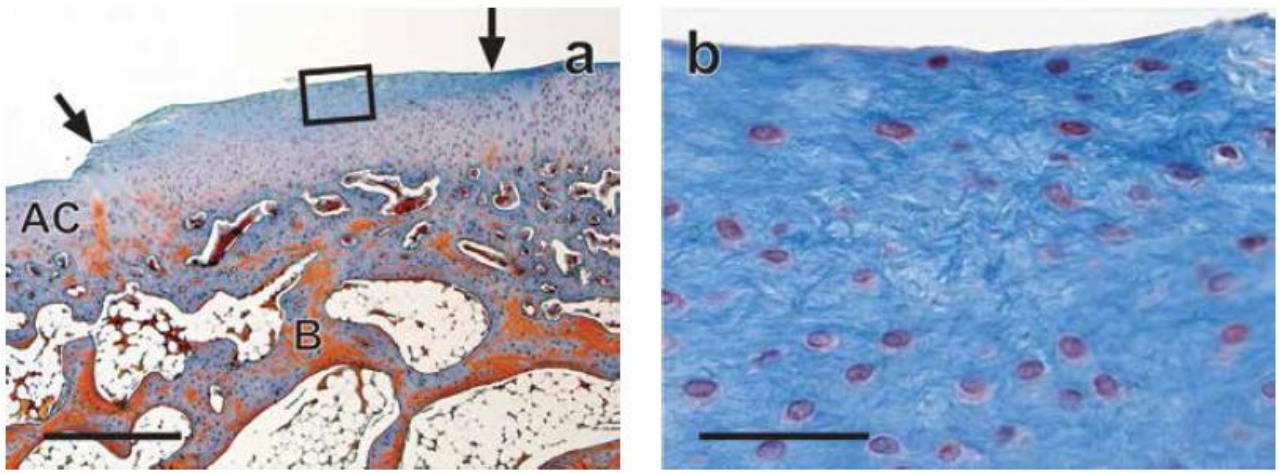

Fig. 11 - Control sample 3 months after surgery, where no scaffold was implanted, showed the appearance of fibrous cartilage filling the excavated cavity (edges indicated by **arrows**; **b**, inset). 5-micron sections were stained with Masson's trichrome. AC = articular cartilage; B = subchondral bone. Scale bars represent 500 μm **(a)** or 100 μm **(b)**.

DISCUSSION

Articular cartilage repair was obtained after 3 months of biostable scaffold implantation in femoral condyle in 2-month-old New Zealand white rabbits. We studied macroscopic and microscopic time evolution of the articular repair, from 1 week to 12 months, combining the creation of a full-thickness cartilage defect, injuring subchondral bone, and the implantation of empty or preseeded scaffolds made of P(EA-co-HEA) copolymers, a synthetic biocompatible biostable polymer. Interestingly, along with articular cartilage repair, the scaffold implanted shifted over time from articular surface towards subchondral bone, and 12 months after implantation it was finally located at a great distance from the surface.

New Zealand white rabbit model has been frequently used in cartilage regenerative studies. These animals were selected due to their docile nature and medium size, thus facilitating care and handling, and because the repair processes produce results relatively quickly as rabbits have a short half-life. Moreover, a minimal immunologic response has been reported when standard rabbit allogeneic chondrocytes were transplanted (31). Although rabbit knee articular cartilage presents some morphological and biomechanical differences with respect to human, it has biological aspects similar to human, and thus the model is considered as suitable for our study (30).

In the present study, we have injured subchondral bone before implanting scaffolds, allowing blood to flow and provide mesenchymal cells to the injury zone. Different techniques are used to injury subchondral bone, such as abrasion chondroplasty, Pridie drilling, spongialization and microfracture (6-8), producing bleeding in the zone of osteoarthritic lesion and clot formation, that initiate bone marrow stem cells migration and thus the regenerative process. These techniques take the advantage of the body's own healing potential (8), representing an easy, simple, minimally invasive, low-morbidity, single-stage procedure, and it has been reported to be cost-effective, associated with few complications, with a high capacity for creation of durable repair tissue, and with best long-

term results in younger active patients with isolated small lesions (13). However, while microfracture remains the first choice for treatment of small cartilage defects, for larger defects, older individuals, and in the long-term, the generation of defect-filling biomaterials is introduced in order to circumvent fragility and loss of the therapeutic superclot from the defect (11, 13).

We have studied long-term articular cartilage repair since short and mid-term cartilage regeneration have been widely studied using different approaches, but few long-term studies using scaffold implantation in full-thickness defects have been reported (11). Sellers and collaborators observed an improvement in the histological appearance and composition of the extracellular matrix 1 year after implantation of collagen sponge impregnated with Bone Morphogenetic Protein-2 (42), whereas Shapiro et al. (41) described the formation of lamellar subchondral bone 6 months after surgery, similar to our results.

Articular cartilage repair

Histologically, articular cartilage is a hyaline cartilage divided into four zones, distinguished by the shape of the chondrocytes and the composition of extracellular matrix including the arrangement of collagen fibers (3, 4, 43), as shown in Figure 12. The superficial zone (SZ) is characterized by small-flattened chondrocytes, low proteoglycan content, and densely packed, horizontally arranged collagen fibrils of uniform diameter. In the middle or transitional zone (MZ), chondrocytes acquire a more rounded profile, proteoglycan content increases, and thick collagen fibers decussate to provide an oblique transitional network between the superficial and deeper zones. The radial zone (RZ) is characterized by spheroid chondrocytes arranged in columns, high proteoglycan content between radially oriented thick collagen bundles. A microscopically distinct line - the tidemark (T) - separates the lower radial zone from the underlying calcified cartilage zone (CZ), which lies above the subchondral bone.

Adult articular cartilage has very low ability of self-repair (3), though it has an active proliferation during prenatal development, which decreases precipitously after birth in New Zealand white rabbits, and undergoes a process of fundamental reorganization during the first 3 months of postnatal period. Thus, a rapidly proliferating cell population is present in articular cartilage of 2-month-old rabbits (5), located in the middle and upper radial zones (transit-amplifying cells), enlarging epiphysis not only in a longitudinal direction, but also radially and laterally (4). Therefore, proliferation and reorganization of neotissue should

occur in the animals used in the present study, either in the presence or the absence of scaffold, and in fact control animals (in which no scaffolds were implanted) showed the ability to produce newly formed tissue but with the structure of fibrous cartilage, in good agreement with the literature, which can be distinguished under the microscope since hyaline cartilage show an homogeneous extracellular matrix (Fig. 12), whereas collagen fibers are easily distinguished in the fibrous one (Fig. 11b).

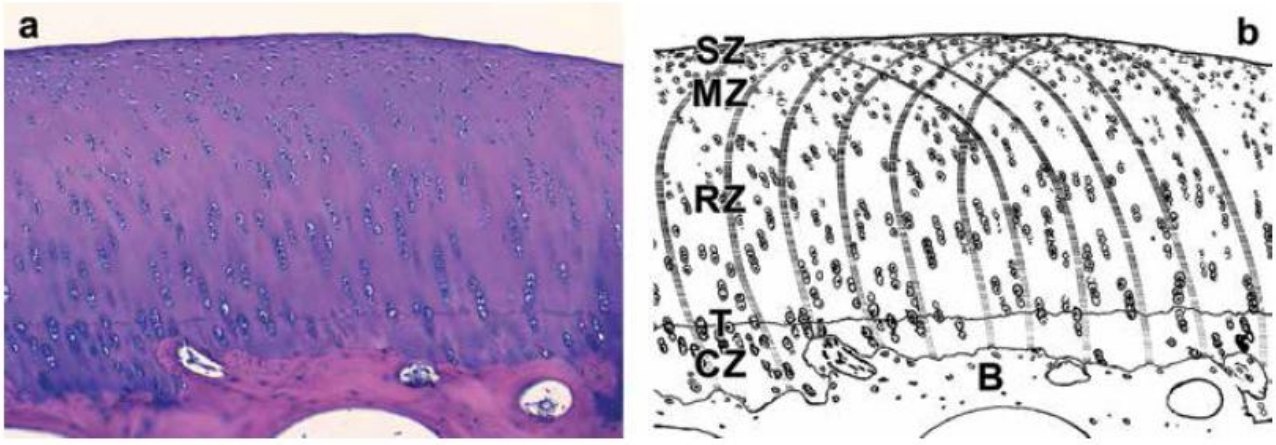

Fig. 12 - Histological structure **(a)** and schematic diagram **(b)** of healthy articular cartilage. Superficial zone (SZ), middle zone (MZ), radial zone (RZ), tidemark (T) and calcified cartilage zone (CZ) are observed over subchondral bone (B). Five-micron sections were stained with hematoxilin-eosin **(a)**. Collagen fibers architecture is represented in **(b)**. Drawing by William V. Barber.

The repair of articular cartilage we observed agrees with previous studies where hyaline cartilage was regenerated on the top of the scaffolds, using similar protocol but with different biomaterials (30), suggesting that the fast growth of this tissue layer had embed the scaffold towards the subchondral bone. In fact, in the early stages after implantation we observe a large number of chondrocytes in many lacunae of the surrounding native cartilage, that later on synthesize cartilaginous matrix, originating the overall growth of the articular cartilage. However, Shapiro et al. (41) demonstrated that residual adjacent articular cartilage did not participate in the repopulation of the defect, but unlike our study, they did not implant any scaffold in the defect.

Although, as stated above, an excellent cartilage repair observed 1 year after surgery, it must be partly due to the age of the animals at the time of surgery (2 months), when cartilage reorganization is still very active (4). However, young age was not enough for cartilage regeneration, since the absence of scaffold highly influenced its functionality, and originated cartilage growth but with a fibrous appearance in control animals.

Mechanical stress support

The function of articular cartilage is intimately linked to biomechanics, since it performs the function of load support and lubrication with minimal wear and little or no damage in animals and humans (1). Thus, biomaterial scaffolds should, on the one hand, provide the chondrogenic cells with a microenvironment where they survive, multiply and produce extracellular matrix to constitute regenerated cartilage (1, 44), and, on the other hand, scaffolds should have mechanical properties matching those of native cartilage (15, 16). On this basis, we used P(EA-co-HEA) copolymer with 5% weight TEGDMA as cross-linker, in order to have a Young's modulus similar to those of native cartilage. Increasing the amount of TEGMA would produce a rise of the Young's modulus, but also brittle material, whereas less amount of TEGMA would produce a weaker material.

The scaffold material used in the present study is biostable and thus it remains almost unaltered 12 months after implantation. Therefore, scaffolds are biomechanically active throughout the regenerative process, and the cells within scaffold pores are subjected to compression stresses similar to those suffered by the chondrocytes of healthy tissue (44), which is important in the differentiation process of chondrocytes in order to acquire the phenotype of hyaline cartilage cells (45).

In previous studies we used scaffolds made of polycaprolactone, empty or preseeded with cultured chondrocytes, and we observed that defects were filled with cartilaginous tissue 3 months after implantation in a similar way than in the present study (30), suggesting that the mechanical role of the scaffold is to provide a substrate that helps the transfer of the compressive stresses to the newly formed tissue.

However, when subchondral bone was injured but no scaffold was implanted (control animals), the repaired articular cartilage 3 months after surgery was not hyaline cartilage but fibrous, in good agreement with previous studies (30, 41), as well as with a long-term study by Hunziker and Rosenberg who observed the appearance of fibrous connective tissue 1 year after an articular cartilage defect that was filled only with mitogenic factors or with cells (46). This result suggests the importance of the mechanical transduction operated by the scaffold to favor an adequate biomechanical environment of the repaired tissue.

The cells located on the surface of the scaffold, aligned with the articular surface, are subjected to compressive loading that directs the extracellular matrix organization and probably plays an important role in chondrogenic differentiation through mechanotransductive pathways. This biomechanical environment is maintained while the

cartilage surface layer grows pushing the scaffold into subchondral bone. The presence of the scaffold is also crucial to initiate bone remodeling at the places where it contacts and transmit compression loading to subchondral bone (47). Therefore, although the ability of cartilage repair is not entirely lost at this age, our results suggest that the scaffold plays a key role in stress transmission to the cells, which is a clue factor in cell phenotype maintenance and tissue organization.

Neotissue growth within scaffolds

Scaffold pores were invaded by mesenchymal cells that proliferated and morphologically differentiated to cartilaginous or bone tissues 3 months after implantation, in agreement with other studies (41, 48), as well as with similar studies that used scaffolds made of different materials in the presence or absence of preseeded chondrocytes (30, 32).
The origin of cells that colonize the scaffolds can vary. The main cellular source is the outflowing bone marrow blood that contains pluripotent stem cells, which are established by the clot formation in the defect, providing an enriched environment for tissue regeneration, making them a potential cell source in cartilage repair (2, 8, 11).
Mesenchymal cells arrival to the injured zone could lead to cartilage regeneration if a number of circumstances occur (13), such as: initial cell recruitment to the injury site; cell adhesion to a local matrix followed by activation and extensive cell proliferation; cell switch to chondrogenic matrix production, whose composition changes during the differentiation of mesenchymal cells into chondrocytes (49); integration with neighboring tissue; and finally regeneration of a tidemark, adaptation to biomechanical loading and building up a balance tissue homeostasis.
Synovium is also a potential source of mesenchymal cells for clinical applications. It has been shown that synovial-derived mesenchymal cells had great ability for chondrogenesis, suggesting that they may be a more attractive source for cartilage repair than bone marrow (46, 50, 51), and therefore they can be partly responsible for the repair observed in the present study.
Cartilage integration in the surrounding tissue is one of the major problems that limit the efficacy of cartilage repair (46). The porous architecture of the scaffolds used in the present study facilitates its integration with adjacent cartilage and subchondral bone tissues, besides providing a favorable environment for neotissue proliferation, migration and differentiation state maintenance. In the present study, we observed that scaffolds were well anchored to the adjacent host tissue 3 months after implantation in most cases,

which can be attributed to the ingrowths and remodeling of surrounding tissue into the scaffold. Different results have been shown in similar studies, for instance Schaefer and collaborators reported that bone tissue also showed a good integration whereas cartilage did not (52), and Wang et al. reported a better surrounding cartilage infusion (32). These results are probably due to the differences of the material used and the age of the rabbits at the time of surgery.

We compared tissue repair 3 months after surgery to an additional group where scaffolds were preseeded with allogenic chondrocytes before implantation. Preseeded scaffolds showed no qualitative differences with respect to the non-preseeded ones at the same time after implantation, although the amount of tissue grown within the scaffolds seemed greater when the scaffolds were preseeded with cultured chondrocytes, which agrees with other studies where similar protocols were followed (30).

Autologous chondrocytes transplantation is a suitable technique for improving the rate of repair of large articular cartilage defects (48). However, this technique requires cell obtaining from a donor and sufficient cell expansion, which can be accompanied by chondrocyte dedifferentiation with the production a non-hyaline cartilaginous mechanically inferior extracellular cartilage matrix (48); therefore special care should be taken in maintaining chondrocyte (re)differentiation in order to obtain chondral matrix. Thus, since superficial cartilage repair, neotissue growth and integration with the surroundings showed only slight differences between non-preseeded and preseeded scaffolds at the age studied, we suggest that the use of the preseeded materials is outbalanced by the far more complicated and risky procedure.

CONCLUSIONS

Articular cartilage repair was studied throughout one year, after a biostable scaffold was implanted in a cavity performed in the femoral trochlea groove, along with subchondral bone injury. Superficial articular cartilage regenerated 3 months after implantation, with the appearance of hyaline-like cartilage covering scaffolds that were progressively pushed towards subchondral bone, whereas good integration with surrounding tissues was observed. However, controls (without scaffold implantation) resulted in a fibrous cartilage. Tissue grown within the scaffold pores was slightly improved when preseeded scaffolds were used. The results strongly suggest the importance of scaffold in stress transmission to cells in order to guide cartilage repair for therapeutically human use.

ACKNOWLEDGEMENTS

The authors want to acknowledge Roberto García Gómez for the technical assistance in the preparation of polymer scaffolds, José Benavent for the histological techniques and William V. Barber for the drawing and graphic support.

REFERENCES

1. Becerra J, Andrades JA, Guerado E, Zamora-Navas P, López-Puertas JM, Reddi AH. Articular cartilage: structure and regeneration. Tissue Eng Part B Rev. 2010; 16(6):617-627.
2. Nelson L, Fairclough J, Archer CW. Use of stem cells in the biological repair of articular cartilage. Expert Opin Biol Ther. 2010; 10(1):43-55.
3. Mainil-Varlet P, Aigner T, Brittberg M, et al. Histological assessment of cartilage repair: a report by the Histology Endpoint Committee of the International Cartilage Repair Society (ICRS). J Bone Joint Surg Am. 2003; 85-A(Suppl 2):45-57.
4. Hunziker EB, Kapfinger E, Geiss J. The structural architecture of adult mammalian articular cartilage evolves by a synchronized process of tissue resorption and neoformation during postnatal development. Osteoarthritis Cartilage. 2007; 15(4):403-413.
5. Onyekwelu I, Goldring MB, Hidaka C. Chondrogenesis, joint formation, and articular cartilage regeneration. J Cell Biochem. 2009; 107(3):383-392.
6. Ahmed TA, Hincke MT. Strategies for articular cartilage lesion repair and functional restoration. Tissue Eng Part B Rev. 2010; 16(3):305-329.
7. Insall J. The Pridie debridement operation for osteoarthritis of the knee. Clin Orthop Relat Res. 1974; 101:61-67.
8. Steadman JR, Rodkey WG, Briggs KK, Rodrigo JJ. The microfracture technic in the management of complete cartilage defects in the knee joint. Orthopade. 1999; 28(1):26-32.
9. Hangody L, Kish G, Kárpáti Z, Udvarhelyi I, Szigeti I, Bély M. Mosaicplasty for the treatment of articular cartilage defects: application in clinical practice. Orthopedics. 1998; 21(7):751-756.
10. Minas T, Nehrer S. Current concepts in the treatment of articular cartilage defects. Orthopedics. 1997; 20(6):525-538.

11. Steinwachs MR, Guggi T, Kreuz PC. Marrow stimulation techniques. Injury. 2008; 39(Suppl 1):S26-S31.
12. Brittberg M, Lindahl A, Nilsson A, Ohlsson C, Isaksson O, Peterson L. Treatment of deep cartilage defects in the knee with autologous chondrocyte transplantation. N Engl J Med. 1994; 331(14):889-895.
13. Richter W. Mesenchymal stem cells and cartilage in situ regeneration. J Intern Med. 2009; 266(4):390-405.
14. Bartlett W, Skinner JA, Gooding CR, et al. Autologous chondrocyte implantation versus matrix-induced autologous chondrocyte implantation for osteochondral defects of the knee: a prospective, randomised study. J Bone Joint Surg Br. 2005; 87(5):640-645.
15. Little CJ, Bawolin NK, Chen X. Mechanical properties of natural cartilage and tissue-engineered constructs. Tissue Eng Part B Rev. 2011; 17(4):213-227.
16. Vikingsson L, Gallego Ferrer G, Gómez-Tejedor JA, Gómez Ribelles JL. An "in vitro" experimental model to predict the mechanical behavior of macroporous scaffolds implanted in articular cartilage. J Mech Behav Biomed Mater. 2014; 32:125-31.
17. Weber JF, Waldman SD. Calcium signaling as a novel method to optimize the biosynthetic response of chondrocytes to dynamic mechanical loading. Biomech Model Mechanobiol. 2014; 13(6):1387-1397.
18. Mauck RL, Soltz MA, Wang CC, et al. Functional tissue engineering of articular cartilage through dynamic loading of chondrocyte-seeded agarose gels. J Biomech Eng. 2000; 122(3):252-260.
19. Palmoski MJ, Brandt KD. Effects of static and cyclic compressive loading on articular cartilage plugs in vitro. Arthritis Rheum. 1984; 27(6):675-681.
20. Khoshgoftar M, Ito K, van Donkelaar CC. The influence of cell-matrix attachment and matrix development on the micromechanical environment of the chondrocyte in tissue-engineered cartilage. Tissue Eng Part A. 2014; 20(23-24):3112-3121.
21. Agrawal CM, Ray RB. Biodegradable polymeric scaffolds for musculoskeletal tissue engineering. J Biomed Mater Res. 2001; 55(2):141-150.
22. Li WJ, Danielson KG, Alexander PG, Tuan RS. Biological response of chondrocytes cultured in three-dimensional nanofibrous poly(epsilon-caprolactone) scaffolds. J Biomed Mater Res Part A. 2003; 67(4):1105-1114.
23. Pérez Olmedilla M, Garcia-Giralt N, Pradas MM, et al. Response of human chondrocytes to a non-uniform distribution of hydrophilic domains on poly (ethyl

acrylate-co-hydroxyethyl methacrylate) copolymers. Biomaterials. 2006; 27(7):1003-1012.

24. Horbett TA, Schway MB. Correlations between mouse 3T3 cell spreading and serum fibronectin adsorption on glass and hydroxyethylmethacrylate-ethylmethacrylate copolymers. J Biomed Mater Res. 1988; 22(9):763-793.
25. Kiremitçi M, Peşmen A, Pulat M, Gürhan I. Relationship of surface characteristics to cellular attachment in PU and PHEMA. J Biomater Appl. 1993; 7(3):250-264.
26. Lydon MJ, Minett TW, Tighe BJ. Cellular interactions with synthetic polymer surfaces in culture. Biomaterials. 1985; 6(6):396-402.
27. Campillo-Fernandez AJ, Pastor S, Abad-Collado M, et al. Future design of a new keratoprosthesis. Physical and biological analysis of polymeric substrates for epithelial cell growth. Biomacromolecules. 2007; 8(8):2429-2436.
28. Funayama A, Niki Y, Matsumoto H, et al. Repair of full-thickness articular cartilage defects using injectable type II collagen gel embedded with cultured chondrocytes in a rabbit model. J Orthop Sci. 2008; 13(3):225-232.
29. Kitahara S, Nakagawa K, Sah RL, et al. In vivo maturation of scaffold-free engineered articular cartilage on hydroxyapatite. Tissue Eng Part A. 2008; 14(11):1905-1913.
30. Martinez-Diaz S, Garcia-Giralt N, Lebourg M, et al. In vivo evaluation of 3-dimensional polycaprolactone scaffolds for cartilage repair in rabbits. Am J Sports Med. 2010; 38(3):509-519.
31. Masuoka K, Asazuma T, Ishihara M, et al. Tissue engineering of articular cartilage using an allograft of cultured chondrocytes in a membrane-sealed atelocollagen honeycomb-shaped scaffold (ACHMS scaffold). J Biomed Mater Res B Appl Biomater. 2005; 75(1):177-184.
32. Wang Y, Bian YZ, Wu Q, Chen GQ. Evaluation of three-dimensional scaffolds prepared from poly(3-hydroxybutyrate-co-3-hydroxyhexanoate) for growth of allogeneic chondrocytes for cartilage repair in rabbits. Biomaterials. 2008; 29(19):2858-2868.
33. Gómez Ribelles JL, Monleón Pradas M, García Gómez R, Forriol F, Sancho-Tello M, Carda C. The role of three-dimensional scaffolds in the regeneration of joint cartilage. In: Fred A, Filipe J, Gamboa H, eds. Biodevices 2010. Portugal: INSTICC, 2010; 229-234.

34. Alió Del Barrio JL, Chiesa M, Gallego Ferrer G, et al. Biointegration of corneal macroporous membranes based on poly(ethyl acrylate) copolymers in an experimental animal model. J Biomed Mater Res A. 2015; 103(3):1106-1118.
35. Martínez-Ramos C, Vallés-Lluch A, Verdugo JM, et al. Channeled scaffolds implanted in adult rat brain. J Biomed Mater Res A. 2012; 100(12):3276-3286.
36. Diego RB, Olmedilla MP, Aroca AS, et al. Acrylic scaffolds with interconnected spherical pores and controlled hydrophilicity for tissue engineering. J Mater Sci Mater Med. 2005; 16(8):693-698.
37. Serrano Aroca A, Campillo Fernández AJ, Gómez Ribelles JL, Monleón Pradas M, Gallego Ferrer G, Pissis P. Porous poly(2-hydroxyethyl acrylate) hydrogels prepared by radical polymerisation with methanol as diluent. Polymer. 2004; 45:8949-8955.
38. Diani J, Fayolle B, Gilormini P. A review on the Mullins effect. Eur Pol J. 2009; 45(3):601-612.
39. Mullins L. Softening of rubber by deformation. Rubber Chem Technol. 1969; 42(1):339-362.
40. Jurvelin JS, Buschmann MD, Hunziker EB. Mechanical anisotropy of the human knee articular cartilage in compression. Proc Inst Mech Eng H. 2003; 217(3):215-219.
41. Shapiro F, Koide S, Glimcher MJ. Cell origin and differentiation in the repair of full-thickness defects of articular cartilage. J Bone Joint Surg Am. 1993; 75(4):532-553.
42. Sellers RS, Zhang R, Glasson SS, et al. Repair of articular cartilage defects one year after treatment with recombinant human bone morphogenetic protein-2 (rhBMP-2). J Bone Joint Surg Am. 2000; 82(2):151-160.
43. Hunziker EB, Michel M, Studer D. Ultrastructure of adult human articular cartilage matrix after cryotechnical processing. Microsc Res Tech. 1997; 37:271-284.
44. Appelman TP, Mizrahim J, Elisseeff JH, Seliktar D. The differential effect of scaffold composition and architecture on chondrocyte response to mechanical stimulation. Biomaterials. 2009; 30(4):518-525.
45. Chung C, Burdick JA. Engineering cartilage tissue. Adv Drug Deliv Rev. 2008; 60(2):243-262.
46. Hunziker EB, Rosenberg LC. Repair of partial-thickness defects in articular cartilage: cell recruitment from the synovial membrane. J Bone Joint Surg. 1996; 78(5):721-733.
47. Maher SA, Doty SB, Torzilli PA, et al. Nondegradable hydrogels for the treatment of focal cartilage defects. J Biomed Mater Res A. 2007; 83(1):145-155.

48. Schulze-Tanzil G. Activation and dedifferentiation of chondrocytes: implications in cartilage injury and repair. Ann Anat. 2009; 191(4):325-338.
49. Umlauf D, Frank S, Pap T, Bertrand J. Cartilage biology, pathology and repair. Cell Mol Life Sci. 2010; 67(24):4197-4211.
50. Karystinou A, Dell'Accio F, Kurth TB, et al. Distinct mesenchymal progenitor cell subsets in the adult human synovium. Rheumatology. 2009; 48(9):1057-1064.
51. Sakaguchi Y, Sekiya I, Yagishita K, Muneta T. Comparison of human stem cells derived from various mesenchymal tissues: superiority of synovium as a cell source. Arthritis Rheum. 2005; 52(8):2521-2529.
52. Schaefer D, Martin I, Jundt G, et al. Tissue-engineered composites for the repair of large osteochondral defects. Arthritis Rheum. 2002; 46(9):2524-2534.

NOMENCLATURE / ABBREVIATIONS

DMEM	Dulbecco's modified Eagle's medium
EA	ethyl acrylate
FBS	fetal bovine serum
HEA	hydroxyethyl acrylate
PBS	phosphate buffered saline
P(EA-co-HEA)	ethyl acrylate and hydroxyethyl acrylate copolymer
PMMA	poly(ethyl methacrylate)
TEGDMA	triethylenglycoldimethacrylate
UV	ultraviolet